Alteration of regional stress by reservoirs and other inhomogeneities: stabilizing or destabilizing?

Modification des contraintes régionales due à la présence de réservoirs et autres hétérogénéitiés: facteur de stabilité ou d'instabilité?

Veränderung des regionalen Spannungszustandes durch Reservoire und andere Inhomogenitäten: Stabilisierung oder Instabilisierung?

J. W. Rudnicki, Northwestern University, Evanston, Illinois, USA

(misprints, corrected December 20, 2004)

in *Proceedings of the Ninth International Congress on Rock Mechanics*, Paris, France, August 25-28, edited by G. Vouille and P. Berest, Vol. 3, pp. 1629- 1637, 1999.

ABSTRACT: The solution of Eshelby (1957) is used to calculate the alteration of regional stress by a reservoir or other region with elastic constants, pore pressure, or temperature different than the surrounding material. As the aspect ratio of the inhomogeneity, the ratio of thickness to lateral extent, approaches zero, the local strain change approaches uniaxial plus the imposed far field (regional) strain. The approach to uniaxial strain with decreasing aspect ratio is slower if the shear modulus of the inhomogeneity exceeds that of the surrounding material. Depletion or withdrawal stress paths in a space of shear stress vs. effective mean stress are steeper for flatter reservoirs, smaller reservoir Poisson's ratios, smaller ratios of reservoir shear modulus to matrix shear modulus and bigger ς, Biot's porous media constant. Generally, steeper stress paths cause the reservoir stress state to move toward failure for injection and away from failure for withdrawal.

RÉSUMÉ: La solution d'Eshelby (1957) est utilisée afin de calculer l'altération des contraintes régionales due à un réservoir ou à toute autre région dont les constantes élastiques, la pression de pore ou la température diffèrent du milieu environnant. La déformation, superposée à la déformation imposée à grande distance, est presque uni-axiale lorsque le rapport épaisseur sur longueur horizontale de l'hétérogénéité tend vers zéro. Le taux de convergence de cette limite est moins marqué lorsque le module d'élasticité en cisaillement de l'hétérogénéité est plus grand que celui du milieu environnant. Les chemins de contrainte lors d'une réduction de pression ou d'un retrait dans l'espace contrainte de cisaillement contrainte effective moyenne sont de plus fortes pentes pour des réservoirs de moindres épaisseurs, pour des coefficients de Poisson plus petits dans le réservoir , pour des rapports module d'élasticité en cisaillement dans le réservoir et à l'extérieur plus petits et pour de plus grandes valeurs de zeta, constante de Biot des milieux poreux. De façon générale, les chemins de plus grandes pentes conduisent à des états de contrainte proches de la ruine pour l'injection et les éloignent de cette ruine pour des retraits.

ZUSAMMENFASSUNG: Eshelby's (1957) Lösung für das Spannungsfeld um eine elastische Inhomogenität erlaubt die Berechnung der durch ein poroelastisches "Reservoir" oder ähnliches Gebiet hervorgerufenen Spannungsänderung, wenn sich dieses Gebiet in den elastischen Konstanten, Porendruck, oder Temperatur von seiner Umgebung unterscheidet. Wenn das Verhältnis von Mächtigkeit zu lateraler Ausdehnung einer solchen Inhomogenität gegen Null geht, nähert sich die lokale Verformungsänderung innerhalb der Inhomogenität einem uniaxialen Verzerrungszustand. Diese Annäherung an den uniaxialen Verzerrungszustand mit abnehmender Mächtigkeit verläuft langsamer, wenn der Schubmodul der Inhomogenität grösser als der der Umgebung ist. Stellt man produktionsbedingte Änderungen der Schubspannung als Funktion der mittleren effektiven Druckspannung dar, so ist deren Verlauf desto steiler, je geringer die Mächtigkeit des Reservoirs, je kleiner dessen Poissonzahl und Schubmodul (im Verhältnis zu dem der Umgebung) und je grösser die Biot Konstante zeta. Allgemein gilt: Ein steilerer Spannungspfad verschiebt den Spannungszustand innerhalb der Inhomogenität bei zunehmendem Porendruck (Injektion) in Richtung Scherbruch, während bei abnehmendem Porendruck (Produktion) die Spannungen vom Bruchzustand abrücken.

1 INTRODUCTION

The stress and strain in reservoirs, aquifers, intrusions, fault zones and other inhomogeneities can differ significantly from the regional fields because the elastic response, pore pressure or temperature in the inhomogeneity generally differs from that of the surrounding material. Of particular interest are the stress and strain changes in a reservoir due to a change in pore pressure accompanying injection or withdrawal of fluid mass. Although the strain state induced in the reservoir is commonly assumed to be uniaxial, Teufel et al. (1991) have questioned the validity of this assumption. In addition, Segall & Fitzgerald (1998) have noted that the concomitant prediction of no horizontal strain above the reservoir disagrees with field observations. Uniaxial strain is shown here to be a good approximation for a thin inhomogeneity, having thickness much less than lateral extent. But, even when the elastic properties of the inhomogeneity are identical to those of the surrounding material, the change of stress and strain in the inhomogeneity due to a fluid pressure change depends on its geometry.

The well-known solution of Eshelby (1957) is exploited to explore the effects of geometry and elastic property mismatch on altering the local stress state. The inhomogeneity is idealized as ellipsoidal in shape with different elastic properties than the surrounding material. Although geological structures may seldom be exactly ellipsoidal, this geometry encompasses a wide range of possible shapes, from spherical to layer-like, in the limit of an ellipsoid with one principal axis much smaller than the other two. In addition, the inhomogeneity is assumed to be hydraulically and thermally isolated so that its temperature and pore pressure may differ from the surrounding material.

The inhomogeneity is assumed to be embedded in an infinite elastic solid. This will be a good approximation for inhomogeneities in the crust for which the depth is greater than the lateral extent. For shallower inhomogeneities, corrections for the effect of the free surface may be needed but the solution for the infinite body still indicates the dependence on shape and properties. Segall & Fitzgerald (1998) have used this model to examine stresses induced in hydrocarbon and geothermal reservoirs but consider the reservoir properties to be identical to those of the surrounding material.

For a given far field stress or strain state, corresponding to regional values, or a change of pressure and temperature in the inhomogeneity, the stress and strain within the inhomogeneity are

easily determined from Eshelby's solution. Thus, the local slope of the stress path for fluid injection or withdrawal can be calculated. This slope together with a failure condition in terms of the stress, e.g. the Mohr-Coulomb criterion, determines whether the stress alteration is stabilizing or destabilizing in the sense of causing the inhomogeneity stress state to move toward or away from failure. Failure of a reservoir, or other inhomogeneity, may be associated with seismicity or enhanced cracking that alters the permeability.

2 FORMULATION

2.1 *Eshelby Solution*

A region ("the inclusion") of a uniform, infinite elastic solid undergoes a change of size and shape that, in the absence of the constraint of the surrounding material, could be described by a uniform transformation strain ε^T_{ij}. If the inclusion is ellipsoidal, then Eshelby (1957) demonstrated that the actual constrained strain ε^C_{ij}, which results in the presence of the constraint of the surrounding matrix, is also uniform and is related to the transformation strain by

$$\varepsilon^C_{ij} = S_{ijkl}\varepsilon^T_{kl} \tag{1}$$

where the factors S_{ijkl}, given by Eshelby (1957), depend only on the geometry of the inclusion and Poisson's ratio. Since the strain ε^T_{ij} occurs in the absence of the constraint of the matrix and causes no stress, the stress in the inclusion is given by

$$\sigma^I_{ij} = L_{ijkl}(\varepsilon^I_{kl} - \varepsilon^T_{kl}) \tag{2}$$

where

$$L_{ijkl} = (K - \tfrac{2}{3}G)\delta_{ij}\delta_{kl} + G(\delta_{ik}\delta_{jl} + \delta_{il}\delta_{jk}) \tag{3}$$

is the tensor of elastic constants for an isotropic solid, K is the bulk modulus, G is the shear modulus and δ_{ij} is the Kronecker delta (δ_{ij} =1, if $i = j$; $\delta_{ij} = 0$, if $i \neq j$). Alternatively, the bulk modulus can be expressed in terms of G and Poisson's ratio ν:

$$K = \tfrac{2}{3}G(1+\nu)/(1-2\nu) \tag{4}$$

The transformation strain can be eliminated from (1) using (2) to yield

$$S_{pqmn}C_{mnij}\sigma^I_{ij} = S_{pqmn}\varepsilon^I_{mn} - \varepsilon^I_{pq} \tag{5}$$

where C_{ijkl} is the tensor of elastic compliances, inverse to L_{ijkl}, satisfying

$$C_{mnij}L_{ijkl} = \frac{1}{2}\left(\delta_{mk}\delta_{nl} + \delta_{ml}\delta_{nk}\right) \tag{6}$$

For an isotropic solid with moduli given by (3), the compliance tensor is

$$C_{ijkl} = \frac{1}{2G}\left\{\tfrac{1}{2}(\delta_{il}\delta_{jk} + \delta_{ik}\delta_{jl}) - \left[\nu/(1+\nu)\right]\delta_{ij}\delta_{kl}\right\} \tag{7}$$

The relation (5) is a consequence of the constraint of the elastic material surrounding the inclusion and is independent of the actual properties of the inclusion (so long as they are homogeneous). To interpret this relation in another way, consider an ellipsoidal cavity subjected to a traction $n_i\sigma^I_{ij}$ at the boundary (n_i are components of the unit normal). The deformation of the boundary, obtained by solving the exterior elasticity problem, is compatible with a uniform strain of the interior given by ε^I_{ij}, where σ^I_{ij} and ε^I_{ij} satisfy (5). In other words, the inclusion (or cavity) can be replaced by material with different properties so long as the traction on the boundary of the ellipsoid and the deformation of the boundary satisfy (5). For any homogeneous material, the transformation strain can always be chosen such that this is the case. Consequently, as recognized by Eshelby (1957), (5) also provides the solution to the problem of an ellipsoidal "inhomogeneity." Rudnicki (1977) has exploited this property of the solution to examine the stability of strain-weakening fault zone.

If the solid surrounding the inhomogeneity is linear poroelastic rather than simply linear elastic, the relation (5) will not, in general, pertain. The response of such a poroelastic solid does, however, reduce to that of an ordinary linear elastic solid in the limits of drained (no change in pore pressure) or undrained (no change in fluid mass content) deformation. Although the elastic moduli in these two limits are different, either could be used in (2) or (5). When neither drained nor undrained conditions pertain, an analogous time-dependent relation could be derived, in principle, from solution of the problem outlined above for an ellipsoidal cavity: Sudden application of a uniform traction at the cavity boundary. In addition, it is necessary to specify whether the cavity boundary is permeable or impermeable. If the boundary of the cavity is found to deform in a manner compatible with a uniform strain of the interior, then a time-dependent relation analogous to (5) can be used to solve the inhomogeneity problem. To my knowledge, this has been done only for a spherical cavity (Rice et al., 1978).

If the solid is loaded by far field strains ε^∞_{ij} related to stresses σ^∞_{ij} by

$$\varepsilon^\infty_{ij} = C_{ijkl}\sigma^\infty_{kl} \tag{8}$$

then (5) applies to the difference of the inclusion values from the farfield values. Replacing σ^I_{ij} and ε^I_{ij} in (5) by the differences (σ^I_{ij} - σ^∞_{ij}) and (ε^I_{ij} - ε^∞_{ij}), respectively, yields

$$S_{mnkl}C_{klij}\left\{\sigma^I_{ij} - \sigma^\infty_{ij}\right\} = \left\{S_{mnkl} - \delta_{mk}\delta_{nl}\right\}\left(\varepsilon^I_{kl} - \varepsilon^\infty_{kl}\right) \tag{9}$$

2.2 *Poroelastic Inhomogeneity*

Here, the inhomogeneity is assumed to be elastic and isotropic, but with elastic constants and pore pressure differing from the surrounding material:

$$\sigma^I_{ij} = L^I_{ijkl}\varepsilon^I_{kl} + \zeta^I p^I \delta_{ij} \tag{10}$$

where L^I_{ijkl} is given by (3) with the subscript I affixed to G and K, ζ^I is a porous media constant (often denoted α and equal to $1-K_I/K'_s$, where K'_s can, under appropriate circumstances, be identified with the bulk modulus of the solid constituents (Rice & Cleary, 1976)), p^I is the pore pressure in the inhomogeneity (measured relative to ambient in the formation) and the form of (10) is appropriate for stresses that are positive in compression. Temperature changes can also be included by appending the term $K_I\,\alpha'_s\Delta\theta\delta_{ij}$ to the right hand side of (10), where α'_s is the cubical thermal expansion coefficient and $\Delta\theta$ is the temperature difference.

Equations (8) and (10) can be used to eliminate the stresses from (9). The result is the following relation between the induced inhomogeneity strain ε^I_{ij}, the imposed far field strain ε^∞_{ij} and the alteration in pore pressure p^I:

$$\varepsilon^I_{mn} + S_{mnkk}\tfrac{1}{3}(k-g)e^I + gS_{mnkl}\varepsilon^I_{kl} = \varepsilon^\infty_{mn} - \tfrac{1}{3}\frac{\zeta^I}{K_\infty}p^I S_{mnkk} \tag{11}$$

where $e^I = \varepsilon^\infty_{kk} = \varepsilon^\infty_{11} + \varepsilon^\infty_{22} + \varepsilon^\infty_{33}$ is the inhomogeneity volume strain, $g = G_I/G_\infty - 1$, $k = K_I/K_\infty - 1$ and the subscript ∞ is now used to designate moduli for the surrounding material. If the far field strains ε^∞_{mn} and the inhomogeneity excess pore pressure p^I are prescribed, then (11) is a system of six equations for the inhomogeneity strain components. If the coordinate directions are aligned with the principal axes of the ellipsoid, the only nonzero members of S_{ijkl} have the form S_{iiii}, S_{jjjj} or S_{ijij} (no sum here on i

or *j*).Consequently, for $m \neq n$, (11) can be solved explicitly for the inhomogeneity shear strain

$$\varepsilon^I_{mn} = \varepsilon^\infty_{mn} \frac{1}{1+2gS_{mnmn}}, \ (m \neq n, \text{ no sum on } m,n) \tag{12}$$

If the shear moduli of the inhomogeneity and the matrix are equal (g = 0), (11) uncouples and the normal strain can also be determined directly. In general, however, the normal strains (and pore pressure) are coupled by three equations.

Alternatively, the strains can be eliminated from (9), resulting in the following relation between the far field and inclusion stresses:

$$\begin{aligned} &\sigma^I_{rs} + L^I_{rsmn} S_{mnkl} \left\{ C^\infty_{klpq} - C^I_{klpq} \right\} \sigma^I_{pq} \\ &\quad = L^I_{rsmn} C^\infty_{mnpq} \sigma^\infty_{pq} + \zeta^I p^I \left\{ \delta_{rs} - L^I_{rsmn} S_{mnkl} C^I_{klpp} \right\} \end{aligned} \tag{13}$$

When this expression is specialized to isotropic materials and the stresses are separated into deviatoric and spherical parts, i.e.

$$\sigma_{ij} = s_{ij} + \tfrac{1}{3}\sigma_{kk}\delta_{ij} \tag{14}$$

the result is the following two equations:

$$\begin{aligned} &s^I_{mn} + g\left\{ S_{mnkl} - \frac{S_{ppkl}\left[kS_{mnqq} + \delta_{mn}\right]}{3(1+\alpha k)} \right\} s^I_{kl} \\ &= (1+g)s^\infty_{mn} - \frac{2G_I}{3K_\infty} \frac{\left[S_{mnkk} - \alpha\delta_{mn}\right]}{(1+\alpha k)} \left(\zeta^I p^I + k\sigma^\infty \right) \\ &\sigma^I (1+\alpha k) + g\left(K_I / 2G_I\right) S_{mmkl} s^I_{kl} = (1+k)\sigma^\infty + (1-\alpha)\zeta^I p^I \end{aligned} \tag{15}$$

where $3\alpha = S_{mmkk} = (1 + \nu_\infty)/(1 - \nu_\infty)$.

3 SPECIAL CASES

3.1 *Spherical Inhomogeneity*

A spherical inhomogeneity may be an appropriate shape for a few geological applications, perhaps, some aquifers or intrusive bodies, but is more significant as an illuminating limiting case. For a spherical inhomogeneity, the shape factors have the following form:

$$S_{mnpq} = \tfrac{1}{2}\beta(\delta_{pm}\delta_{qn} + \delta_{pn}\delta_{qm}) + \tfrac{1}{3}\delta_{mn}\delta_{pq}(\alpha - \beta) \tag{16}$$

where $\beta = 2(4–5\nu_\infty)\ /15(1–\nu_\infty)$. The solution for the inhomogeneity strains is as follows:

$$\varepsilon^I_{mn} = \frac{\varepsilon^\infty_{mn} - \delta_{mn}e^\infty}{1+\beta g} + \frac{\delta_{mn}}{1+\alpha k}\left(e^\infty - \frac{\alpha\zeta^I p^I}{3K_\infty} \right) \tag{17}$$

If the deviatoric portion of the far field strain is zero, the first term in (17) vanishes and the inhomogeneity strains are purely volumetric. Conversely, if the far field volume strain and the pore pressure difference are zero, then the second term vanishes and the inhomogeneity strains are purely deviatoric.

3.2 *Thin, Axisymmetric Inhomogeneity*

An axisymmetric inhomogeneity is frequently a good approximation for the shape of aquifers or reservoirs. If the principal semi-axes are $a = b$ and c, the aspect ratio of the inhomogeneity is $e = c/a$. If the ellipsoid is thin ($e << 1$) and the distinguished axis is labeled 3, the only shape factors that do not vanish in the limit $e \rightarrow 0$ are

$$\begin{aligned} 2S_{2323} &= 2S_{1313} = 1 - \frac{\pi}{4}\frac{(2-\nu_\infty)}{(1-\nu_\infty)}e + \ldots \\ S_{3333} &= 1 - \frac{\pi}{4}\frac{(1-2\nu_\infty)}{(1-\nu_\infty)}e + \ldots \\ S_{3311} &= S_{3322} = \frac{\nu_\infty}{(1-\nu_\infty)} - \frac{\pi}{8}\frac{(1+4\nu_\infty)}{(1-\nu_\infty)}e + \ldots \end{aligned} \tag{18}$$

To zeroth order in the aspect ratio, the inhomogeneity strains are

$$\begin{aligned} \varepsilon^I_{\kappa\gamma} &= \varepsilon^\infty_{\kappa\gamma} \\ \varepsilon^I_{\kappa 3} &= \varepsilon^\infty_{\kappa 3}(G_I/G_\infty)^{-1} \\ \varepsilon^I_{33} &= \frac{\varepsilon^\infty_{33} - \alpha(\zeta^I p^I/K_\infty) + \frac{1}{2}(\varepsilon^\infty_{11} + \varepsilon^\infty_{22})\left\{g(1-\alpha) - 2\alpha k\right\}}{1 + (1-\alpha)g + \alpha k} \end{aligned} \tag{19}$$

where $(\kappa, \gamma) = (1,2)$. Thus, the difference between the inhomogeneity strains and the imposed regional strains is a purely uniaxial field.

3.3 *Strain Ratios for Uniaxial Farfield Strain*

To illustrate the dependence of the inhomogeneity strain on the property mismatch and geometry, consider the case of an axisymmetric inhomogeneity subjected to far field uniaxial strain (only $\varepsilon^\infty_{33} \neq 0$, and zero pore pressure difference, $p^I = 0$). Uniaxial strain is often regarded to be a good approximation if the region under consideration has lateral extent much greater than its depth. If the material is elastic this approximation implies that the ratio of the lateral to vertical stress is $\nu_\infty/(1 - \nu_\infty)$, but measurements tend to indicate that the lateral stress is greater than this (McGarr & Gay, 1978). If the 3-axis is taken to be vertical, the ratio of the lateral to vertical strain increments in the inhomogeneity, $R = \Delta\varepsilon^I_{11}/\ \Delta\varepsilon^I_{33}$, is given by

$$R = -\frac{kS_{11kk} + g(3S_{1133} - S_{11kk})}{3 + 2kS_{11kk} - g(3S_{1133} - S_{11kk})} \tag{20}$$

where

$$S_{1133} = \frac{1}{4(1-\nu_\infty)}\left\{ \frac{e^2(2-3I(e))}{(1-e^2)} - (1-2\nu_\infty)I(e) \right\} \tag{21}$$

$$I(e) = \frac{e}{(1-e^2)^{3/2}}\left\{ \arccos(e) - e(1-e^2)^{1/2} \right\} \tag{22}$$

and $S_{11kk} = (3\alpha/2)\ I(e)$.The ratio R equals zero for uniaxial strain, –1/2 for equivoluminal strain and unity for purely voluminal strain.

Figures 1, 2 and 3 plot R against the inhomogeneity Poisson's ratio υ_I for various combinations of the other parameters. In Figure 1, $\nu_\infty = 0.2$, $G_I/G_\infty = 1.0$ and results are shown for five values of e: 0.1, 0.2, 0.4, 0.6 and 1; in Figure 2, $e = 0.2$, $G_I/G_\infty = 1.0$ and results are shown for five values of ν_∞: 0.0, 0.1, 0.2, 0.3, and 0.4;. in Figure 3, $e = 0.2$, $\nu_\infty = 0.2$, and results are shown for five values of G_I/G_∞: 0.2, 0.5, 1.0, 2.0 and 5.0 For a thin inhomogeneity, $e = 0.0$, $R = 0$ regardless of the value of the Poisson's ratios. In all cases, $R \rightarrow –0.5$, equivoluminal deformation, as $\upsilon_I \rightarrow 0.5$

Figures 1 and 2 indicate that for $G_I = G_\infty$ and $\nu_I < \nu_\infty$, $R > 0$, meaning that $\Delta\varepsilon_{11}$ and $\Delta\varepsilon_{33}$ have the same sign but $R < 0$ for $\nu_I > \nu_\infty$. In addition, Figures 1 and 2 indicate that the magnitude of R increases with aspect ratio and with ν_∞. Figure 3 shows that the magnitude increases with $G_I\ /\ G_\infty$. Note, however, from Figure 3, that for small values of $G_I\ /\ G_\infty$, R can be negative even when $\nu_I < \nu_\infty$.

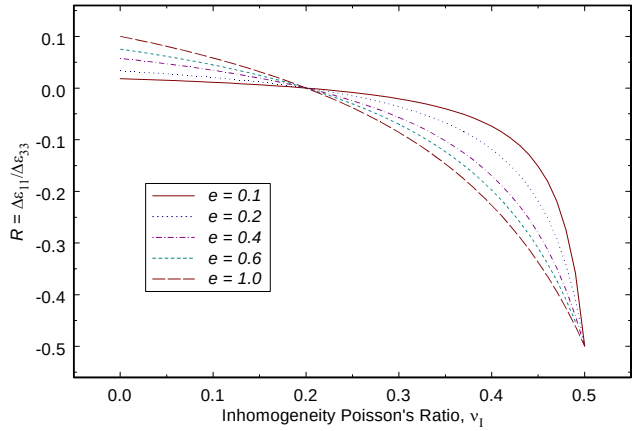

Figure 1. Ratio of strain induced in an inhomogeneity for far field uniaxial strain against Poisson's ratio of inhomogeneity for different aspect ratios *e*.

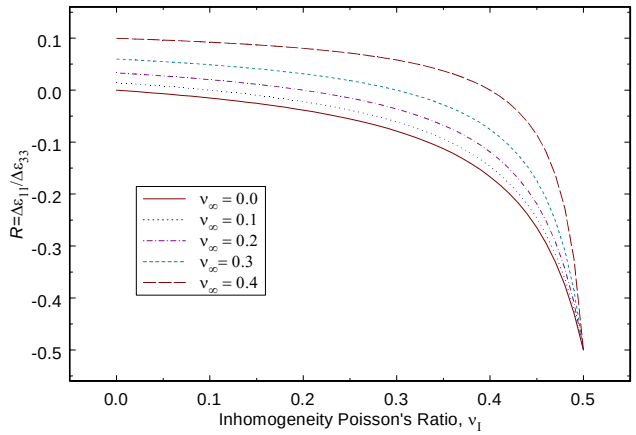

Figure 2. Same as Figure 1 but for different values of ν_∞.

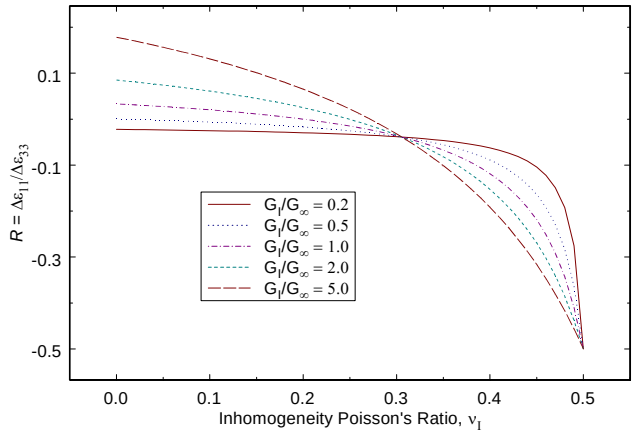

Figure 3. Same as Figure 1 but for different ratios of shear moduli.

4 FLUID WITHDRAWAL OR INJECTION

A relevant application of the above formulation is the injection or withdrawal of fluid from a reservoir or aquifer on a time scale that is rapid by comparison with processes of tectonic strain. In this case, the far field strain can be taken as constant and, hence, $\varepsilon^{\infty}_{mn} = 0$. The strain that would occur in the reservoir in the absence of constraint by the surrounding material (transformation strain) is

$$\varepsilon_{11}^T = \varepsilon_{22}^T = \varepsilon_{33}^T = -\zeta^I p^I / K_I \tag{23}$$

equal all round compression (pressure decrease) or dilation (pressure increase), where p^I is the pore pressure change due to fluid mass alteration (Alternatively, the transformation strain can be expressed directly in terms of the fluid mass change). The resulting strain in the presence of the constraint of the matrix depends on the geometry of the reservoir and the property mismatch. For an axisymmetric reservoir (again with the 3-axis distinguished), the ratio of lateral (ε^I_{11}) to axial (ε^I_{33}) strain increments is given by the following expression

$$R = \frac{3\alpha - S_{33kk} + g\left\{3\alpha S_{3333} - S_{33kk}S_{pp33}\right\}}{2S_{33kk} + g\left\{3\alpha S_{3333} - S_{33kk}S_{pp33}\right\}} \tag{24}$$

where

$$\begin{aligned} S_{3333} &= 1 - \frac{(1-2\nu_\infty)}{2(1-\nu_\infty)} I(e) - \frac{e^2(2-3I(e))}{2(1-\nu_\infty)(1-e^2)} \\ S_{kk33} &= 1 - \frac{(1-2\nu_\infty)}{(1-\nu_\infty)} I(e) \\ S_{33kk} &= \frac{(1+\nu_\infty)}{(1-\nu_\infty)}(1-I(e)) \end{aligned} \tag{25}$$

and *I(e)* is given by (22). In addition the axial strain ε_{33} can be written as

$$\varepsilon_{33} = -\frac{\zeta^I p^I}{K_I} E_3 \tag{26}$$

where

$$E_3 = \frac{\alpha(1+k)}{(1+2R)(1+\alpha k) + g(1-R)(S_{kk33} - \alpha)} \tag{27}$$

Figure 4 plots R against $e = c/a$, for five values of the ratio of reservoir shear modulus to formation shear modulus G_I/G_∞: 0.2, 0.5, 1.0, 2.0 and 5.0 ($\nu_\infty = 0.2$ but the dependence on ν_∞ is weak). As demonstrated by Figure 4, the strain state in thin reservoirs ($e \ll 1$) is constrained to be nearly uniaxial ($R = 0$) but the approach to uniaxial strain with decreasing e is slower for larger values of G_I/G_∞.

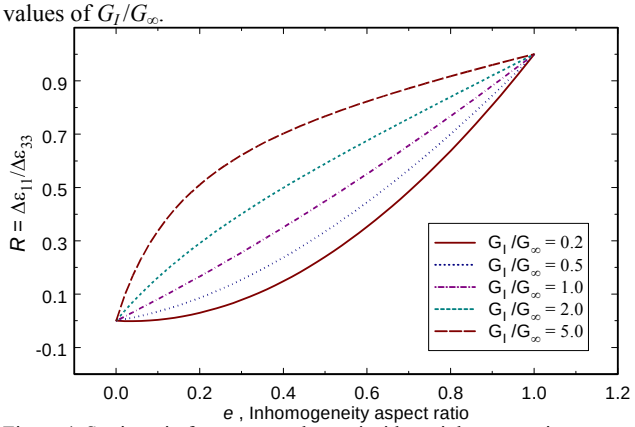

Figure 4. Strain ratio for pressure change inside an inhomogeneity.

Figures 5 and 6 plot E_3 against the aspect ratio e for different ratios of G_I/G_∞ (Figure 5) and different values of the inclusion Poisson's ratio ν_I (Figure 6). The results for E_3 do not depend on ν_∞. Since E_3, as shown in Figures 5 and 6, is positive, the axial strain increment $\Delta\varepsilon_{33}$ is extensional for pressure increase and contractant for pressure decrease. In the limit, $e \to 0$, E_3 approaches the value given by (19) and, for $e \to 1$, E_3 approaches the value given by (17). Figures 5 and 6 demonstrate that the magnitude of the axial strain increases with decreasing aspect ratio for fixed G_I/G_∞ and ν_I. The magnitude also increases with ν_I for fixed G_I/G_∞ (Figure 6) and with G_I/G_∞ for fixed ν_I and larger aspect ratios (Figure 5); for smaller aspect ratios the dependence on G_I/G_∞ is more complex because the approach to uniaxial strain is slower for larger G_I/G_∞.

The stress components can be determined from (10) in terms of R (24) and E_3 (27). The axial stress increment is

$$\Delta\sigma_{33}^I = \varsigma^I \Delta p^I \left\{1 - E_3(1+2R) - E_3(1-R)\frac{2(1-2\nu_I)}{(1+\nu_I)}\right\} \tag{28}$$

and the lateral stress increment is

$$\Delta\sigma_{11}^I = \varsigma^I \Delta p^I \left\{1 - E_3(1+2R) + E_3(1-R)\frac{(1-2\nu_I)}{(1+\nu_I)}\right\} \tag{29}$$

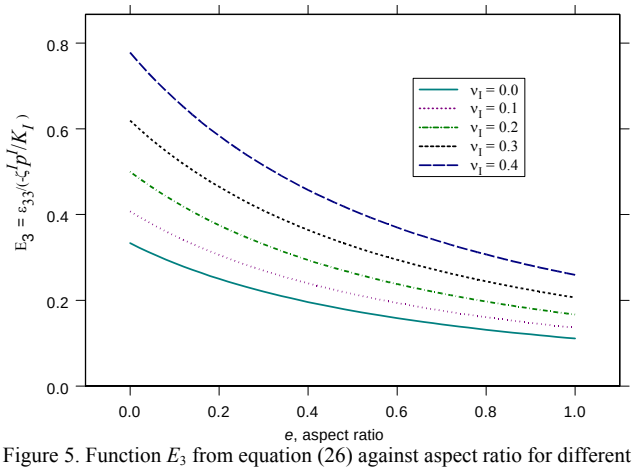

Figure 5. Function E_3 from equation (26) against aspect ratio for different values of the inhomogeneity Poisson's ratio.

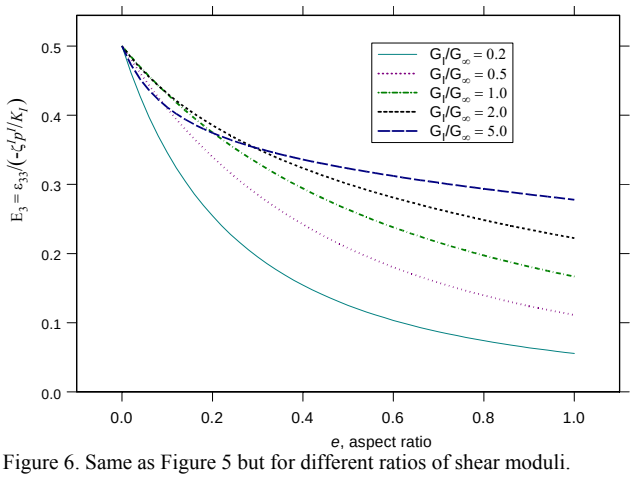

Figure 6. Same as Figure 5 but for different ratios of shear moduli.

Figures 7 and 8 show the axial and lateral stress components, divided by $\zeta^I p^I$, against the aspect ratio e. In Figure 7, $\nu_I = 0.2$, and results are shown for three values of modulus ratio G_I/G_∞: 0.2, 1.0, and 5.0; in Figure 8, $G_I/G_\infty = 1.0$ and results are shown for $\nu_I = 0.0$, 0.2 and 0.4. Both stress components are independent of ν_∞. Because the stress components are proportional to the pressure change, they are compressive for injection (increasing p) and tensile for withdrawal (decreasing p). The axial stress change approaches zero as the reservoir becomes thin ($e \to 0$) but the approach is slower for smaller ν_I and, especially, for $G_I/G_\infty < 1.0$, that is, if the reservoir is more compliant than the surrounding material. As $e \to 0$ the horizontal stress approaches $\zeta^I p^I(1-2\nu_I)/(1-\nu_I)$, consistent with uniaxial strain, but the approach is slower if the reservoir is stiffer than the surrounding material ($G_I/G_\infty > 1.0$). As the reservoir shape approaches spherical ($e \to 1$), both stress components approach

$$\sigma_{11}^I = \sigma_{33}^I = \varsigma^I p^I \left\{1 + \frac{G_I}{G_\infty}\frac{(1+\nu_I)}{2(1-2\nu_I)}\right\}^{-1} \tag{30}$$

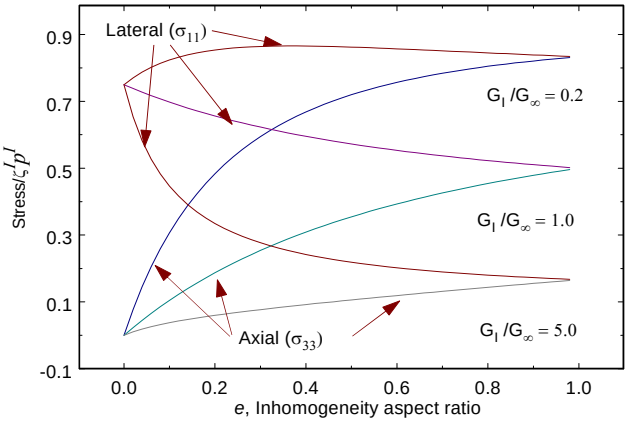

Figure 7. Stress components due to pressure change inside an inhomogeneity, $\nu_I = 0.2$ and $G_I/G_\infty = 0.2$, 1.0, and 5.0.

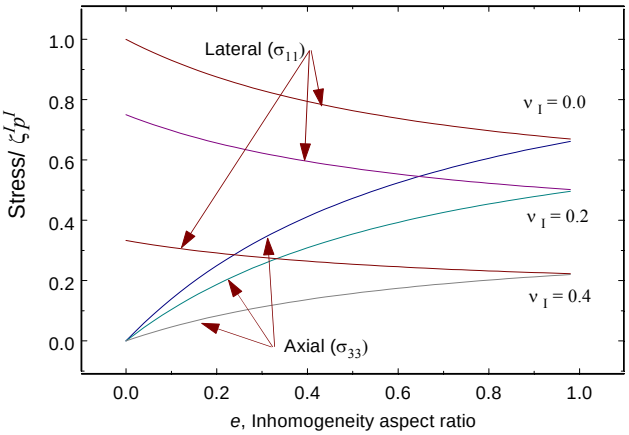

Figure 8. Stress components due to pressure change inside an inhomogeneity, $G_I/G_\infty = 1.0$ and $\nu_I = 0.0$, 0.2, and 0.4.

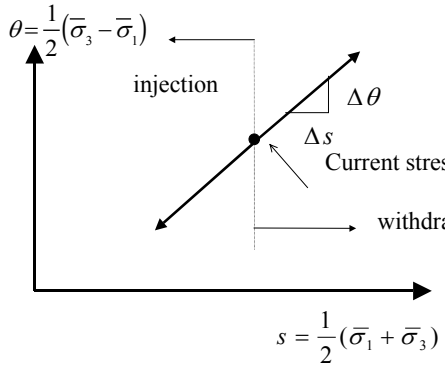

Figure 9. Stress paths for injection and withdrawal.

4.1 *Depletion or Withdrawal Effective Stress Paths*

For an axisymmetric reservoir, the stress path caused by change of pressure can be represented in a plot of q versus s (Figure 9) where $q = (\bar{\sigma}_3 - \bar{\sigma}_1)/2$, $s = (\bar{\sigma}_3 + \bar{\sigma}_1)/2$, σ_3 and σ_1 are the maximum and minimum principal stresses, positive in compression, and $\bar{\sigma}_i = \sigma_i - p$ is the effective stress. Rice (1977) has argued on theoretical grounds that this is the appropriate form of the effective stress for failure and inelasticity governed by microcracking and frictional sliding on surfaces with small real contact areas. In addition, observations are generally consistent with this form (Paterson, 1978). The ratio $\Delta q/\Delta s$ due to a change of pressure can be calculated explicitly from (15) but the result is lengthy and not recorded here. A reasonably compact expression can be obtained by using (24), (26), (27) and (10):

$$\frac{\Delta q}{\Delta s} = \frac{\zeta^I E_3 (G_I / K_I)(1-R)}{1-\zeta^I \left\{1-\left[\frac{3E_3}{2(1+\nu_I)}\right]\left[1+R(1+2\nu_I)\right]\right\}} \tag{31}$$

where R is given by (24) and E_3 by (27). Since the stress components are independent of the Poisson's ratio of the matrix, ν_∞, so is this ratio. For a spherical reservoir, $\Delta q = 0$ and Δs is positive or negative depending on whether the pressure is decreased or increased. Thus, the stress path is horizontal in Figure 9. For a thin reservoir (e <<1), the ratio reduces to

$$\Delta q / \Delta s = \left\{\frac{2(1-\nu_I)}{\zeta^I (1-2\nu_I} - 1\right\}^{-1} \tag{32}$$

Figures 10, 11, and 12 show the slope of the stress path against ν_I, the inhomogeneity Poisson's ratio, for various combinations of the aspect ratio (e), the ratio of reservoir shear modulus to formation shear modulus (G_I/G_∞) and Biot's porous media constant ζ^I. It is evident from these figures that Δq and Δs have the same sign. Since Δs is negative for pressure increase (injection) and positive for pressure decrease (withdrawal), so is Δq. In addition, Figures 10, 11, and 12 demonstrate that the stress paths are steeper (larger $\Delta q/\Delta s$) for smaller e and G_I/G_∞ and larger ζ^I.

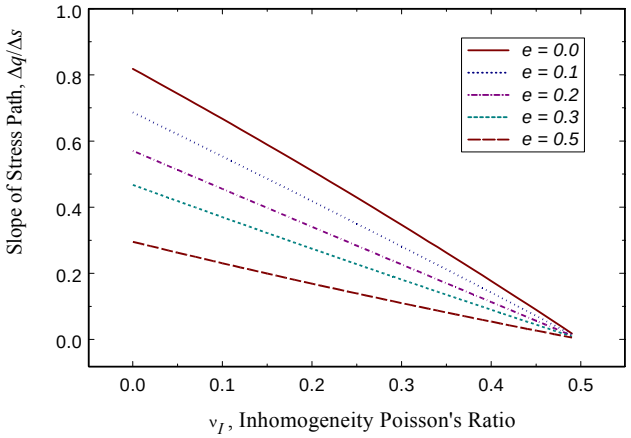

Figure 10. Slope of stress path for $G_I/G_\infty = 1.0$ and $\zeta^I = 0.9$.

4.2 *Temperature Changes*

As noted earlier, the effect of temperature changes can be included by appending a term to the inhomogeneity constitutive relation (10). This addition is incorporated into subsequent expressions and, in particular, the expression for the ratio $\Delta q/\Delta s$ by replacing ζ^I by $\zeta^I + K_I \alpha'_s \Delta\theta/\Delta p$. Since ζ^I is typically between 0.5 and 1.0, the magnitude of $K_I \alpha'_s \Delta\theta/\Delta p$ is a measure of the relative contributions of thermoelasticity and poroelasticity. For K_I = 40 GPa, corresponding to G_I = 30 GPa and ν_I = 0.2, and α'_s= 3.64 x 10^{-5}/°C, the value for quartz, the product $K_I \alpha'_s$ is 1.46 MPa/°C. Thus, the effects of a temperature change of 6.8 °C and a 10 Mpa pressure change are comparable. For increases in pressure (injection), temperature decreases tend to reduce the magnitude of $\Delta q/\Delta s$ and temperature increases tend to increase the magnitude of $\Delta q/\Delta s$. For decreases in pressure (withdrawal), temperature increases tend to reduce the magnitude of $\Delta q/\Delta s$ and temperature increases tend to increase the magnitude of $\Delta q/\Delta s$.

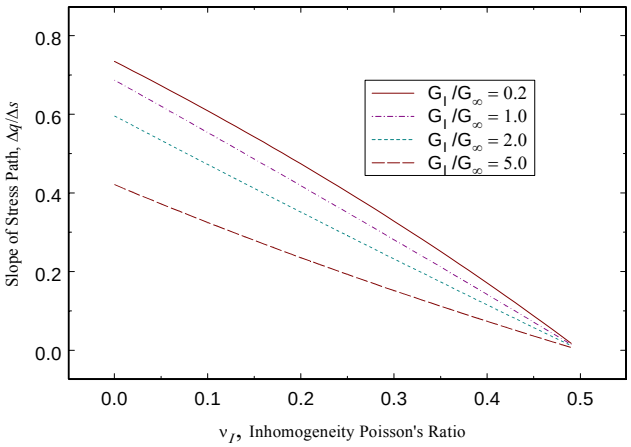

Figure 11. Slope of the stress path for $\zeta^I = 0.9$ and $e = 0.1$.

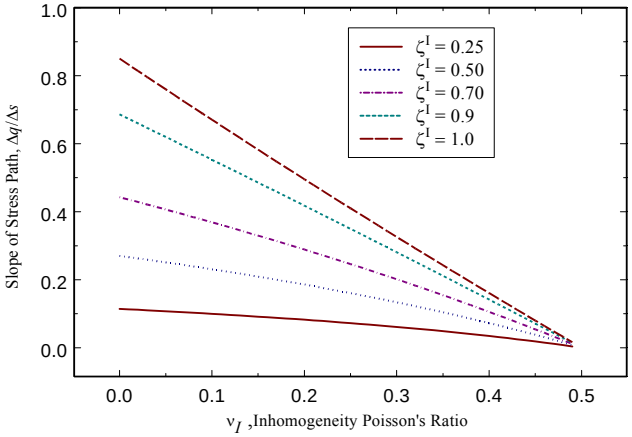

Figure 12. Slope of the stress path for $G_I/G_\infty = 1.0$ and $e = 0.1$.

5 APPROACH TO FAILURE

5.1 *General Formulation*

Since stress changes in the inhomogeneity, due to either pressure alteration or a change of far field stress or strain, can be calculated from (15), these changes can be used to determine whether the change causes the stress state to move closer or further from failure. This approach has been widely applied with the Mohr-Coulomb condition, as will be done in the next section, but here the idea is formulated more generally. Let the failure condition be given by a surface in stress space described by

$$F(\sigma_{ij}) = 0 \tag{33}$$

where $F < 0$ for stress states not at failure. Let σ^0_{ij} be a stress state on the failure surface and consider the conditions for which a small increment of stress $\Delta\sigma_{ij}$ causes the stress state to move inside the failure surface:

$$F(\sigma^0_{ij} + \Delta\sigma_{ij}) < 0 \tag{34}$$

Such an increment will be termed "stable". Since the increment is presumed small, the left hand side of (34) can be expanded to yield

$$F(\sigma^0_{ij}) + \frac{\partial F}{\partial \sigma_{kl}}(\sigma^0_{ij})\Delta\sigma_{kl} + (...) < 0 \tag{35}$$

where (…) stands for terms of order ($\Delta\sigma_{kl}\,\Delta\sigma_{kl}$) or smaller and a repeated subscript implies summation. The terms denoted (…) will be negligible if the curvature of the surface is not too severe and the increment $\Delta\sigma_{ij}$ is small. Since σ^0_{ij} is on the failure sur-

face, the first term is zero and the condition that the stress increment be stable is

$$\frac{\partial F}{\partial \sigma_{kl}}(\sigma_{ij}^0)\Delta\sigma_{kl} < 0 \tag{36}$$

The geometric interpretation of this condition is shown schematically in Figure 13: the projection of the stress increment on the outward normal to the surface (33) (pointing into $F > 0$) is negative or that the stress increment is moving away from the tangent plane of the failure surface.

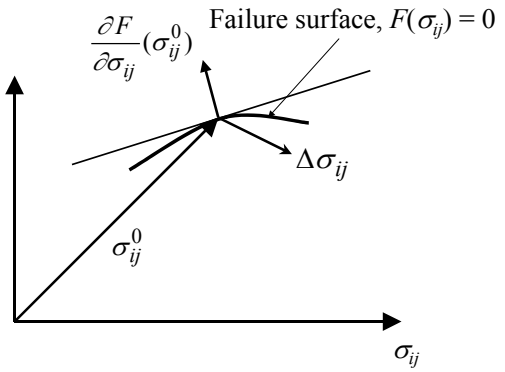

Figure 13. Schematic illustration of stability criterion.

The derivation has assumed that the initial stress state σ^0_{ij} is on the failure surface. But, as long as the distance of the initial stress state from the failure surface is much less than the local radius of curvature, the condition (36) ensures that the stress increment will cause the stress state to move away from the failure surface. If the initial stress state is far from the failure surface, then movement toward the failure surface may be of little concern. If the failure surface is sharply curved then a more elaborate analysis may be needed if σ^0_{ij} is not actually on the surface, but the case of a vertex comprising planar facets could be treated by a minor modification of the approach here.

If the material can be idealized as isotropic with respect to failure, then F in (33) can be expressed in terms of three invariants of the stress state:

$$F(I, J_2, J_3) = 0 \tag{37}$$

where

$$I = tr(\sigma) = \sigma_{11} + \sigma_{22} + \sigma_{33}$$
$$J_2 = \frac{1}{2}s_{ij}s_{ij} \tag{38}$$
$$J_3 = \det(s_{ij}) = \frac{1}{3}s_{ij}s_{jk}s_{ki}$$

For a failure surface described by (33), the stability criterion (36) becomes

$$\left\{\frac{\partial F}{\partial I}\frac{\partial I}{\partial \sigma_{ij}} + \frac{\partial F}{\partial J_2}\frac{\partial J_2}{\partial \sigma_{ij}} + \frac{\partial F}{\partial J_3}\frac{\partial J_3}{\partial \sigma_{ij}}\right\}\Delta\sigma_{ij} < 0 \tag{39}$$

Computing the derivatives of the invariants with respect to the stress, substituting into (39), and separating the stress increment into deviatoric and spherical components yields

$$\left\{\frac{\partial F}{\partial J_2}s_{ij} + \frac{\partial F}{\partial J_3}s_{jk}s_{ki}\right\}\Delta s_{ij} + \frac{\partial F}{\partial I}\Delta\sigma_{kk} < 0 \tag{40}$$

If the stresses are referred to principal axes, (40) can be rewritten as

$$(s_1 - s_2)\left\{\frac{\partial F}{\partial J_2} - s_3\frac{\partial F}{\partial J_3}\right\}\Delta s_1 - (s_2 - s_3)\left\{\frac{\partial F}{\partial J_2} - s_1\frac{\partial F}{\partial J_3}\right\}\Delta s_3 + \frac{\partial F}{\partial I}\Delta I < 0 \tag{41}$$

If the stress increment is axisymmetric, i.e., $\Delta\sigma_1 = \Delta\sigma_2 \neq \Delta\sigma_3$, then $\Delta s_3 = -2\Delta s_1$ and (41) becomes

$$\frac{\partial F}{\partial I}\Delta I < \Delta s_1\left\{3s_3\frac{\partial F}{\partial J_2} + (2s_1s_2 + s_3^2)\frac{\partial F}{\partial J_3}\right\} \tag{42}$$

When the stress increment is axisymmetric, it is more convenient to express the increments in terms of q and s. In this case, $\Delta I = 3\Delta s - \Delta q$ and $\Delta s_1 = -(2/3)\,\Delta q$. If, in addition, the stress state itself is axisymmetric, $s_3 = -2s_1$ and (43) can be written as

$$3\frac{\partial F}{\partial I}\Delta s + \Delta q\left\{2s_3\frac{\partial F}{\partial J_2} + s_3^2\frac{\partial F}{\partial J_3} - \frac{\partial F}{\partial I}\right\} < 0 \tag{43}$$

As a simple example, consider the Drucker-Prager failure condition:

$$\sqrt{3J_2} - (mI + b) = 0 \tag{44}$$

where the form assumes stresses are positive in compression and m and b are positive constants. The condition (43) becomes

$$\Delta q\left(m \pm 2\right) < 3m\Delta\bar{s} \tag{45}$$

where $\Delta\bar{s}$ is the increment in effective stress, that is, the total stress minus pore pressure; the plus sign pertains to axisymmetric compression and the minus to axisymmetric extension. For fluid withdrawal (pressure decrease) both Δq and $\Delta\bar{s}$ are positive and the condition on the slope becomes:

$$\frac{\Delta q}{\Delta\bar{s}} < \frac{3m}{m \pm 2} \tag{46}$$

For injection (pressure increase) both Δq and $\Delta\bar{s}$ are negative; thus, dividing through by $\Delta\bar{s}$ reverses the inequality.

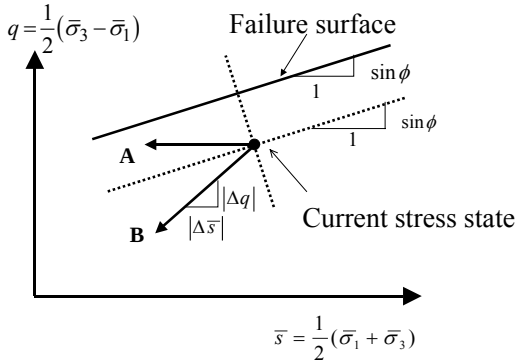

Figure 14. Schematic illustration of stability condition for withdrawal and Mohr-Coulomb failure criterion.

5.2 *Stability of Injection or Withdrawal*

The procedure described in the preceding section is implemented here for the simple, linear Mohr-Coulomb failure criterion:

$$|q| = \bar{s}\sin\varphi + C_0\cos\varphi \tag{47}$$

where φ is the friction angle, C_0 is the cohesion, and q and $\bar{s}$ are defined as previously. (If the stress state is axisymmetric, then

the Drucker-Prager criterion can be written in the same form with

$$\sin\varphi = \frac{3}{2 \pm m}, \text{ and } C_0 \cos\varphi = \frac{b}{2 \pm m} \tag{48}$$

where m and b are the constants in (44).)The slope of the failure surface is sin φ if $\sigma_3 > \sigma_1$ and –sin φ if $\sigma_3 < \sigma_1$. For definiteness, assume that the reservoir or other inhomogeneity is horizontal and flat-lying so the axis, x_3, is vertical and that the vertical stress exceeds the horizontal ($\sigma_3 > \sigma_1$), as appropriate for a normal faulting regime. Then, as depicted in Figure 14, the criterion for stress changes caused by fluid injection to be stable is the following:

$$\frac{\Delta q}{\Delta \bar{s}} > \sin\varphi \tag{49}$$

(Hettema et al. (1998) derive an equivalent condition with the additional assumption that the total vertical stress is constant and the use of the Biot effective stress, $\sigma_{ij} - \varsigma p \delta_{ij}$, rather than $\sigma_{ij} - p\delta_{ij}$, in the failure criterion.) If the pore pressure is increased with the total stresses held constant, $\bar{s}$ is decreased but q remains the same. Thus, the reservoir stress state moves horizontally to the left, as indicated by the arrow A in Figure 14, and, hence, closer to the failure line. Injection does not, however, generally occur at fixed total stress: increasing the reservoir pressure alters the stress state. The stress state will move away from the failure line if (49) is met as indicated by the arrow B in Figure 14.

Hence, for fluid injection (pressure increase), steeper stress paths favor stability (tend to move the stress state away from failure). For example, if φ = 30º, sin φ = 0.5, and stress paths with slopes in excess of this value in Figures 10-12 would be stable; those with smaller values would be unstable. Recall that slopes are larger for smaller aspect ratios e, smaller G_I / G_∞ and larger ζ^I. For injection, temperature decreases reduce the magnitude of $\Delta q / \Delta \bar{s}$ and, hence, are destabilizing; temperature increases are stabilizing.

For fluid withdrawal, corresponding to a decrease in reservoir pressure, $\Delta \bar{s}$ is positive and the direction of the inequality in (49) should be reversed for stability. Thus, for withdrawal, smaller slopes favor stability. From hydraulic fracturing tests in the Ekofisk Field, Teufel et al. (1998) infer a ratio of effective lateral stress to effective vertical stress of about 0.2. This corresponds to $\Delta q / \Delta \bar{s} = 0.67$ and, consistent with their conclusion, (49) suggests the stress path for withdrawal is unstable for friction angles less than 42º.

The preceding discussion has assumed that $\sigma_3 > \sigma_1$ as appropriate for a normal faulting regime. If $\sigma_3 < \sigma_1$, as appropriate for a thrust regime, then considerations similar to the preceding show that injection is always destabilizing and withdrawal is always stabilizing.

6 CONCLUSIONS

The solution of Eshelby (1957) has been used to calculate the stress and strain changes inside an ellipsoidal inhomogeneity due to imposed far field strains or pressure and temperature changes within the inhomogeneity. The material of the inhomogeneity is assumed to be described by a linear, isotropic poro-thermoelastic solid.

Although the analysis is obviously idealized, the inhomogeneity may be a suitable model for a reservoir, aquifer, or, perhaps, a fault zone. If the inhomogeneity is hydraulically and thermally isolated from the surroundings and relatively permeable and conductive, uniform temperature and pore pressure is a reasonable idealization. Reservoirs and aquifers are by their nature hydraulically isolated from the surroundings and this may also be a good approximation for some fault zones. Temperatures and pressures are undoubtedly nonuniform in actual inhomogeneities, and the quantities appearing in this analysis should be regarded as spatial averages over the inhomogeneity.

A further limitation of the analysis is that the inhomogeneity is embedded in an infinite elastic solid. This will be a good approximation for inhomogeneities in the crust having depths greater than the lateral extent and approximate corrections could be made for the influence of the free surface.

Of particular relevance are the stress and strain changes due to alterations in pressure or fluid mass on a time scale for which the regional strains may be assumed constant. Depletion and injection stress paths can be calculated easily. The discussion here has focussed on the effects of geometry and elastic property property mismatch. Note, however, that inelastic deformation, neglected here, will also affect the stress paths. Inelastic deformation could be included approximately by regarding the elastic constants as incremental quantities pertaining to small deviations from the current state.

The calculated stress paths are used to evaluate whether the stress state is moving toward or away from failure. Although this information can be very useful in practical situations a thorough analysis of failure also requires information not only about whether the stress state is moving toward failure but also the distance of the stress state from failure. Considerations of failure can be complicated by the presence of faults within the reservoir or on its boundaries. In additon, the analysis here has focussed on the possibility of failure within the reservoir. Analysis by Segall (1989) has shown that poroelastic deformation caused outside the reservoir by fluid withdrawal can induce seismicity.

In spite of its simplicity, the analysis described can be of practical use when detailed information needed for a more elaborate analysis is unavailable or as a guide to establishing dominant effects, or in making decisions about whether more elaborate analysis is warranted. The simplicity of the approach permits consideration of a wide range of geometries and values of properties. In particular, this approach is an improvement over the seldom suitable assumption that pore pressure changes in a reservoir occur with fixed stress: This would be the case only if the reservoir were unconstrained by the surrounding material. For reservoirs with thickness much less than lateral extent, the analysis demonstrates that the common assumption of uniaxial strain in the reservoir is valid, as long as the shear modulus of the reservoir is not too much larger than that of the surrounding material. Furthermore, the analysis permits quantitative assessment of the geometry and material mismatch for this assumption to be valid and quantitative means of corrections when it is not.

7 ACKNOWLEDGMENTS

Much of this work was motivated by discussions with Nigel Higgs and, in addition, I am grateful to John Logan for many helpful discussions.

REFERENCES

Eshelby, J. D. 1957. The determination of the elastic field of an ellipsoidal inclusion and related problems. *Proceedings of the Royal Society, London* A241: 376-396.

Hettema, M. H. H., Schutjens, P. M. T. M., Verboom, B. J.M., & Gussinklo, H. J., 1998. SPE 50630. In SPE/ISRM Eurock '98 Conference, Trondheim, Norway.

McGarr, A. & Gay, N. C. 1978, State of stress in the earth's crust. *Annual Review of Earth and Planetary Sciences*, 6: 405-436.

Paterson, M. S. Experimental Rock Deformation – The Brittle Field. New York: Springer-Verlag.

Rice, J. R.1978. Pore pressure effects in inelastic constitutive relations for fissured rock masses. In *Advances in Civil Engineering through Engineering Mechanics*: 360-363. New York:American Society of Civil Engineers.

Rice, J. R. & Cleary, M. P. 1976. Some basic stress diffusion solutions for fluid-saturated elastic porous media with compressible constitutents. *Reviews of Geophysics and Space Physics* 14: 227-241.

Rudnicki, J. W. 1977. The inception of faulting in a rock mass with a weakened zone. *Journal of Geophysical Research* 82: 844-854.

Segall, P. 1989. Earthquakes triggered by fluid extraction. *Geology* 17: 942-946.

Segall, P. & Fitzgerald, S. D. 1998. A note on induced stress changes in hydrocarbon and geothermal reservoirs. *Tectonophysics* 289: 117-128.

Teufel, L. W., Rhett, D. W. & Farrell, H. E. 1991. Effect of reservoir depletion and pore pressure drawdown on in situ stress and deformation in the Ekofisk Field, North Sea. In C.-J. Rogiers (ed.), *Rock Mechanics as a Multidisciplinary Science*: 63-72. Rotterdam: Balkema.